

# Solution to the Poisson Boltzmann equation involving various spherical geometries

Rajib Chakraborty\*

Department of Physical Sciences, Indian Institute of Science Education  
and Research Kolkata (IISER-K), Mohanpur-741 246, West Bengal, India

(Dated: May 13, 2019)

The distribution of free charges within fluids or plasma is often modeled using linearized Poisson-Boltzmann equation (PBE). However, this author has recently shown that the usual boundary conditions (BC), namely the Dirichlet condition and the Neumann condition cannot be used to solve the PBE due to some physical reasons. This author has used the BC of ‘mixed’ type to obtain the physical solution to the 1-D PBE and derived the charged density distribution  $\rho_e$  within *rectangular* and *cylindrical* geometries before. Here the 1-D formulae of  $\rho_e$  (i) within, (ii) between and (iii) outside *spherical* geometries has been derived. The result shows that the electric field is high at the surface of small objects, immersed in electrolyte solution. These formulae could be very useful in explaining similar physical situations that are found in nature or made in the laboratories.

**PACS numbers:** 68.08.-p, 94., 82.45.-h, 52.27.Lw

## I. INTRODUCTION

The linearized PBE has been serving as a very important formulation since a long time [1] to find free-charge distribution within ionic solutions or plasma. It is being applied regularly in various branches of physical, chemical and biological sciences, from sub-nanometer to astrophysical scales, e.g. surface chemistry, colloids, micro-nano-fluidics, fusion devices, astrophysical plasmas, radio science, structural biology etc. please see Refs. [2–5] and other references within Ref. [6].

Recently, after some unsuccessful attempts [7, 8] (also see Ref. [9]), we have shown that the old ways of solving the PBE using Dirichlet or Neumann type BCs have serious defects; we addressed these problems and derived new formula for  $\rho_e$  [10, 11]; a minute error in the formula has been corrected in a review process, see Refs. [12, 13].

In Ref. [11] we have derived the expression of  $\rho_e$  for finite rectangular geometry and laid the main physical ideas. In Ref. [6] we derived the expressions of  $\rho_e$  for various cylindrical geometries; we also considered semi-infinite rectangular geometry there; we gave an alternative derivation of  $\rho_e$  for finite rectangular geometry (i.e. the derivation is different from that in Ref. [11]). Here, we derive the formulae of  $\rho_e$  for various *spherical* geometries. In all the above cases (rectangular, cylindrical, spherical), we analyzed 1-D problems only.

## II. SPHERICAL GEOMETRY

See Refs. [14–16] that solved the PBE in spherical geometries. Unlike them, here we have used different BCs to solve the PBE.

In spherical polar coordinate system, a point in space can be represented in various ways, see Ref. [17]; here we use  $(R, \theta, \phi)$  i.e. (radial, polar, azimuthal) system, see section 2.5 of Ref. [18]. The meaning of most of the other symbols can be found in Ref. ([10]), any exception will be notified. First we analyse the domain bounded by two concentric spheres. Then we analyse a pure spherical domain i.e. where the inner sphere is absent.

We consider the problems that depend only on the radial coordinate  $R$ . We use some suitable scales ‘ $a$ ’ and ‘ $\zeta$ ’ (both are positive) for distance and electrostatic potential ( $\psi$ ) respectively. We re-write a few quantities, which were defined in Ref. [6]:

$$r \equiv \frac{R}{a}; \quad \kappa \equiv \left[ \frac{\lambda_D}{a} \right]^{-1}; \quad \psi^* \equiv \frac{\psi}{\zeta}; \quad \rho_0 \equiv \frac{\epsilon \kappa^2 \zeta}{a^2}; \quad \rho_e^* \equiv \frac{\rho_e}{\rho_0} \quad (1)$$

Where,  $\lambda_D$  is the ‘Debye length’,  $\epsilon$  is the permittivity of the fluid.

### A. Charge distribution for a *finite* domain bounded between two concentric spheres

The domain is shown in Fig. 1(a); the ‘inner’ and ‘outer’ radii are  $R_i$  and  $R_o$ , normalized as:  $r_i \equiv R_i/a; r_o \equiv R_o/a$ .

We start with a formula that we derived in Ref. [10] (within its Supplementary Material).

$$\therefore \rho_e^* = -\psi^* \quad (2)$$

Now we define a few quantities, which we will use later. The net charge present in the total domain i.e  $Q_{TOT}$  is given by  $\iiint \rho_e dV$ , where  $dV = R^2 \sin \theta dR d\theta d\phi$ . If  $\rho_e$  depends only upon  $R$ , we have,

$$Q_{TOT} = \int_0^{2\pi} d\phi \int_0^\pi \sin \theta d\theta \int_{R_i}^{R_o} \rho_e R^2 dR = 4\pi \int_{R_i}^{R_o} \rho_e R^2 dR \quad (3)$$

\* mecrajib@gmail.com

Contact address: 89/3 Tanupukur Road, Dhakuria, Calcutta 700031, West Bengal, India

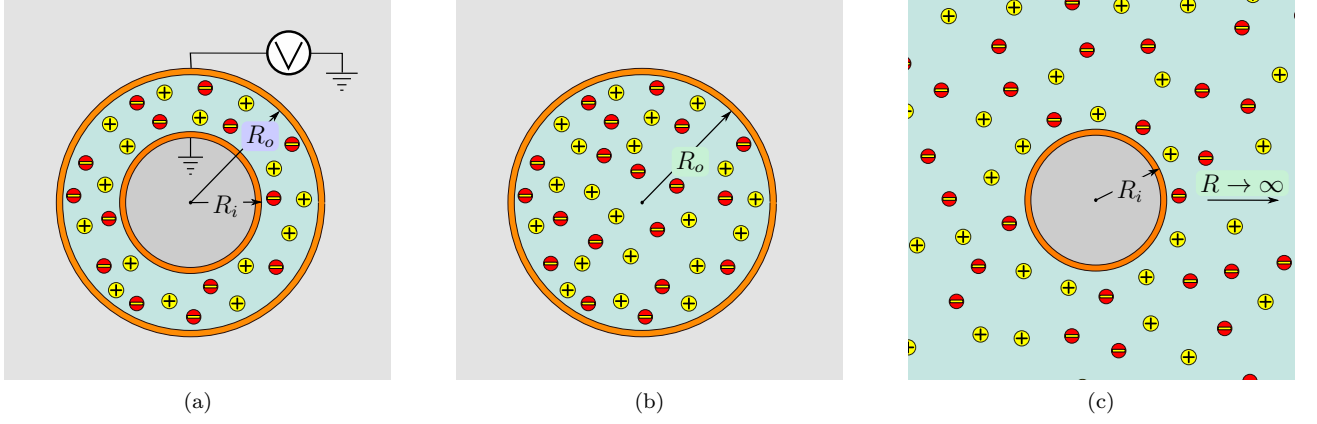


FIG. 1. (Color online) Electrolytic solution bounded by various spherical geometries: sectional views. (a) Between two concentric, finite spheres of radii  $R_i$  and  $R_o$ ; the spheres have a potential difference  $V$ . (b) Within a single, finite sphere of radius  $R_o$  (c) Outside a single, finite sphere of radius  $R_i$ ; the fluid domain extends to infinity. For each case, the +ve and -ve ions shows the corresponding solution domain.

We define a quantity  $Q_{1s}$ , then using Eq. (1) we write its non-dimensional form  $q_{1s}$ ; the subscript ‘1s’ means an 1-D problem in spherical geometry.

$$Q_{1s} \equiv \frac{Q_{TOT}}{4\pi} = \int_{R_i}^{R_o} \rho_e R^2 dR = \rho_0 a^3 \int_{r_i}^{r_o} \rho_e^* r^2 dr \quad (4)$$

$$q_{1s} \equiv \frac{Q_{1s}}{(\rho_0 a^3)} = \int_{r_i}^{r_o} \rho_e^* r^2 dr = - \int_{r_i}^{r_o} \psi^* r^2 dr \quad (5)$$

$Q_{1s}$  is the net charge present in the fluid within a solid-angle of unit steradian, between two spherical surfaces of radii  $R_i$  and  $R_o$ ; it has dimension of ‘charge’ e.g. *Coulomb*, unlike in the rectangular geometry (*Coulomb·meter<sup>-2</sup>*, see Ref. [19]) or cylindrical geometry (*Coulomb·meter<sup>-1</sup>*, see Ref. [6]).

Now,  $\psi$  and  $\rho_e$  are also related by Poisson’s equation in electrostatics (PES), which is given by,

$$\nabla^2 \psi = -\frac{\rho_e}{\epsilon} \quad (6)$$

The expression for  $\nabla^2$  in spherical polar coordinates can be found in section 2.5 of Ref. [18]:

$$\nabla^2 \equiv \frac{1}{R^2} \frac{\partial}{\partial R} \left( R^2 \frac{\partial}{\partial R} \right) + \frac{1}{R^2 \sin \theta} \frac{\partial}{\partial \theta} \left( \sin \theta \frac{\partial}{\partial \theta} \right) + \frac{1}{R^2 \sin^2 \theta} \frac{\partial^2}{\partial \phi^2} \quad (7)$$

In the special case, where  $\psi$  varies only in the ‘radial’ direction, the PES reduces to,

$$\frac{1}{R^2} \frac{d}{dR} \left( R^2 \frac{d\psi}{dR} \right) = -\frac{\rho_e}{\epsilon} \quad (8)$$

using Eq. (1) we first make PES non-dimensional:

$$\begin{aligned} \frac{1}{r^2} \frac{d}{dr} \left( r^2 \frac{d\psi^*}{dr} \right) \left( \frac{\zeta}{a^2} \right) &= -\frac{\rho_0}{\epsilon} \rho_e^* = -\left( \frac{\epsilon \kappa^2 \zeta}{a^2 \epsilon} \right) \rho_e^* \\ \Rightarrow \frac{1}{r^2} \frac{d}{dr} \left( r^2 \frac{d\psi^*}{dr} \right) &= -\kappa^2 \rho_e^* \end{aligned} \quad (9)$$

Using Eq. (2) in Eq. (9) we get non-dimensional PBE in 1-D spherical (radial) coordinates:

$$\frac{1}{r^2} \frac{d}{dr} \left( r^2 \frac{d\psi^*}{dr} \right) = \kappa^2 \psi^* \quad (10)$$

See Ref. [16], the general solution to Eq. (10) is,

$$\psi^* = A \frac{\exp(+\kappa r)}{r} + B \frac{\exp(-\kappa r)}{r} \quad (11)$$

We need two conditions to fix the arbitrary constants  $A$  and  $B$ . We get one condition by integrating PES i.e. Eq. (9) and using Eq. (5),

$$\begin{aligned} \int_{r_i}^{r_o} \left[ \frac{1}{r^2} \frac{d}{dr} \left( r^2 \frac{d\psi^*}{dr} \right) \right] r^2 dr &= -\kappa^2 \int_{r_i}^{r_o} \rho_e^* r^2 dr \\ \Rightarrow \left( r^2 \frac{d\psi^*}{dr} \right) \Big|_{r=r_o} - \left( r^2 \frac{d\psi^*}{dr} \right) \Big|_{r=r_i} &= -q_{1s} \kappa^2 \end{aligned} \quad (12)$$

We assume the potential difference (scaled with  $\zeta$ ) between outer and inner curved boundaries i.e. ‘ $v$ ’ to be known,

$$\psi^*(r_o) - \psi^*(r_i) = v \quad (13)$$

We solve PBE i.e. Eq. (10) using two conditions given by Eq. (12) and Eq. (13).

From Eq. (11) we get,

$$\frac{d\psi^*}{dr} = -\frac{1}{r^2} [A \exp(\kappa r) + B \exp(-\kappa r)] + \frac{\kappa}{r} [A \exp(\kappa r) - B \exp(-\kappa r)] \quad (14)$$

$$\therefore r^2 \frac{d\psi^*}{dr} = - [A \exp(\kappa r) + B \exp(-\kappa r)] + (\kappa r) [A \exp(\kappa r) - B \exp(-\kappa r)] \quad (15)$$

$$= A \exp(\kappa r) [\kappa r - 1] - B \exp(-\kappa r) [\kappa r + 1] \quad (16)$$

Below we write the expression for the radial component of electric field, which will be used later:

$$E_r \equiv -\frac{d\psi^*}{dr} = -\frac{1}{r^2} \left[ A \exp(\kappa r) \{\kappa r - 1\} - B \exp(-\kappa r) \{\kappa r + 1\} \right] \quad (17)$$

From Eq. (12) and Eq. (16) we get,

$$[\exp(\kappa r_o)(\kappa r_o - 1) - \exp(\kappa r_i)(\kappa r_i - 1)] A - [\exp(-\kappa r_o)(\kappa r_o + 1) - \exp(-\kappa r_i)(\kappa r_i + 1)] B = -q_{1s} \kappa^2 \quad (18)$$

From Eq. (11) and Eq. (13) we get,

$$\left[ \frac{\exp(\kappa r_o)}{r_o} - \frac{\exp(\kappa r_i)}{r_i} \right] A + \left[ \frac{\exp(-\kappa r_o)}{r_o} - \frac{\exp(-\kappa r_i)}{r_i} \right] B = v \quad (19)$$

We write Eq. (18) and Eq. (19) together in a compact, matrix form:

$$\begin{pmatrix} C_{11} & C_{12} \\ C_{21} & C_{22} \end{pmatrix} \begin{pmatrix} A \\ B \end{pmatrix} = \begin{pmatrix} d_1 \\ d_2 \end{pmatrix} \quad (20)$$

Where,

$$C_{11} \equiv [\exp(\kappa r_o)(\kappa r_o - 1) - \exp(\kappa r_i)(\kappa r_i - 1)] \quad (21)$$

$$C_{12} \equiv (-1) \times [\exp(-\kappa r_o)(\kappa r_o + 1) - \exp(-\kappa r_i)(\kappa r_i + 1)] \quad (22)$$

$$C_{21} \equiv \left[ \frac{\exp(\kappa r_o)}{r_o} - \frac{\exp(\kappa r_i)}{r_i} \right] \quad (23)$$

$$C_{22} \equiv \left[ \frac{\exp(-\kappa r_o)}{r_o} - \frac{\exp(-\kappa r_i)}{r_i} \right] \quad (24)$$

$$d_1 \equiv -q_{1s} \kappa^2 \quad (25)$$

$$d_2 \equiv v \quad (26)$$

The determinant  $\Delta$  of the above  $2 \times 2$  matrix is given by,

$$\Delta \equiv C_{11} \cdot C_{22} - C_{12} \cdot C_{21} \quad (27)$$

Finally we write  $A$  and  $B$  in terms of known quantities,

$$A = (d_1 \cdot C_{22} - d_2 \cdot C_{12}) / \Delta \quad (28)$$

$$B = (-d_1 \cdot C_{21} + d_2 \cdot C_{11}) / \Delta \quad (29)$$

**With the help of Eq. (28) and Eq. (29), we can use Eq. (11) and Eq. (2) to evaluate  $\psi^*$  and  $\rho_e^*$ .** We can also use an equivalent formula, which is written explicitly in terms of the pair  $(q_{1s}, v)$ . In Eq. (11), we plug in the expressions of  $A$  and  $B$  given by Eq. (28) and Eq. (29) respectively and rearrange terms; then we use Eq. (25), Eq. (26):

$$\psi^* = \frac{1}{\Delta} \left[ (d_1 \cdot C_{22} - d_2 \cdot C_{12}) \frac{\exp(+\kappa r)}{r} + (-d_1 \cdot C_{21} + d_2 \cdot C_{11}) \frac{\exp(-\kappa r)}{r} \right] \quad (30)$$

$$= \frac{1}{\Delta} \left[ d_1 \left\{ C_{22} \frac{\exp(+\kappa r)}{r} - C_{21} \frac{\exp(-\kappa r)}{r} \right\} + d_2 \left\{ -C_{12} \frac{\exp(+\kappa r)}{r} + C_{11} \frac{\exp(-\kappa r)}{r} \right\} \right] \quad (31)$$

$$= \frac{1}{\Delta} \left[ -q_{1s} \kappa^2 \left\{ C_{22} \frac{\exp(+\kappa r)}{r} - C_{21} \frac{\exp(-\kappa r)}{r} \right\} + v \left\{ -C_{12} \frac{\exp(+\kappa r)}{r} + C_{11} \frac{\exp(-\kappa r)}{r} \right\} \right] \quad (32)$$

$$= -\frac{1}{\Delta} \left[ q_{1s} \kappa^2 \left\{ C_{22} \frac{\exp(+\kappa r)}{r} - C_{21} \frac{\exp(-\kappa r)}{r} \right\} + v \left\{ C_{12} \frac{\exp(+\kappa r)}{r} - C_{11} \frac{\exp(-\kappa r)}{r} \right\} \right] \quad (33)$$

Finally we use Eq. (2) i.e.  $\rho_e^* = -\psi^*$ ,

$$\rho_e^* = \frac{1}{\Delta} \left[ q_{1s} \kappa^2 \left\{ C_{22} \frac{\exp(+\kappa r)}{r} - C_{21} \frac{\exp(-\kappa r)}{r} \right\} + v \left\{ C_{12} \frac{\exp(+\kappa r)}{r} - C_{11} \frac{\exp(-\kappa r)}{r} \right\} \right] \quad (34)$$

### B. Charge distribution *within* a single, finite sphere

We consider the charge distribution within a domain bounded by a single sphere of radius  $r_o$  ( $\equiv R_o/a$ ), as shown in Fig. 1(b). This case cannot be considered as a spacial case of the two concentric spheres by just assigning  $r_i = 0$ . Physically they are different as we can still vary the voltage in the double spherical case, but cannot do that for a single sphere. It is mathematically not possible, too, as we cannot assign  $r_i = 0$  in Eq. (23) and Eq. (24), because it leads to division by zero. Hence, we cannot use Eq. (34) for this case of single sphere. Here  $r = 0$  is included in our domain of analysis; it needs special attention. We re-write the general solution to PBE i.e. Eq. (11) in a slightly different way:

$$\psi^* = \frac{[A \exp(+\kappa r) + B \exp(-\kappa r)]}{r} \quad (35)$$

The denominator of Eq. (35) tends to zero as  $r \rightarrow 0$ . However,  $\rho_e^*$  (and hence,  $\psi^*$ ) should not blow up as  $r \rightarrow 0$ , therefore the numerator should also tend to zero as  $r \rightarrow 0$ ; we write,

$$\lim_{r \rightarrow 0} [A \exp(+\kappa r) + B \exp(-\kappa r)] = 0 \quad (36)$$

which gives us  $B = -A$ ; hence,

$$\psi^* = \frac{A[\exp(+\kappa r) - \exp(-\kappa r)]}{r} = 2A \frac{\sinh(\kappa r)}{r} \quad (37)$$

For the special case  $r_i = 0$ , we write  ${}^0q_{1s}$  instead of  $q_{1s}$ . Using Eq. (5), with  $r_i = 0$ , we get,

$$\int_0^{r_o} \psi^* r^2 dr = -{}^0q_{1s} \quad (38)$$

Using the expression of  $\psi^*$  given by Eq. (37) in Eq. (38),

$$\begin{aligned} \int_0^{r_o} \psi^* r^2 dr &= 2A \int_0^{r_o} r \sinh(\kappa r) dr \\ &= 2A \left( \frac{r}{\kappa} \cosh(\kappa r) - \frac{1}{\kappa^2} \sinh(\kappa r) \right) \Big|_0^{r_o} \\ &= \frac{2A}{\kappa^2} [\kappa r_o \cosh(\kappa r_o) - \sinh(\kappa r_o)] = -{}^0q_{1s} \\ \Rightarrow A &= -\frac{{}^0q_{1s} \kappa^2}{2[\kappa r_o \cosh(\kappa r_o) - \sinh(\kappa r_o)]} \quad (39) \end{aligned}$$

We have used the following formula given in Ref. [20]:

$$\int x \sinh(ax) dx = \frac{1}{a} x \cosh(ax) - \frac{1}{a^2} \sinh(ax) + Const. \quad (40)$$

Using Eq. (39) in Eq (37) we get,

$$\psi^* = - \left[ \frac{{}^0q_{1s} \kappa^2}{\kappa r_o \cosh(\kappa r_o) - \sinh(\kappa r_o)} \right] \frac{\sinh(\kappa r)}{r} \quad (41)$$

Eq. (2) i.e.  $\rho_e^* = -\psi^*$  gives,

$$\rho_e^* = \left[ \frac{{}^0q_{1s} \kappa^2}{\kappa r_o \cosh(\kappa r_o) - \sinh(\kappa r_o)} \right] \frac{\sinh(\kappa r)}{r} \quad (42)$$

### C. Charge distribution *outside* a single sphere, in a semi-infinite domain

Here we find the charge distribution outside a single sphere of radius  $r_i$  ( $\equiv R_i/a$ ), immersed in an infinite medium containing free charges; please see Fig. 1(c). In this case, in order to prevent  $\psi^*$  from blowing up as  $r \rightarrow \infty$ , we must set  $A = 0$  in Eq. (11), that equation reduces to,

$$\psi^* = B \frac{\exp(-\kappa r)}{r} \quad (43)$$

For this special case, we set  $r_o = \infty$ , and write  ${}^\infty q_{1s}$  instead of  $q_{1s}$ . Using Eq. (5), with  $r_o = \infty$ , we get,

$$\int_{r_i}^{\infty} \psi^* r^2 dr = -{}^\infty q_{1s} \quad (44)$$

We use the expression of  $\psi^*$  given by Eq. (43) in Eq. (44),

$$\begin{aligned} \int_{r_i}^{\infty} \psi^* r^2 dr &= B \int_{r_i}^{\infty} r \exp(-\kappa r) dr \\ &= B \exp(-\kappa r) \left( \frac{-\kappa r - 1}{\kappa^2} \right) \Big|_{r_i}^{\infty} \\ &= \frac{B}{\kappa^2} (\kappa r_i + 1) \exp(-\kappa r_i) = -{}^\infty q_{1s} \\ \Rightarrow B &= -\frac{{}^\infty q_{1s} \kappa^2}{(\kappa r_i + 1) \exp(-\kappa r_i)} \quad (45) \end{aligned}$$

Using the expression of  $B$  given by Eq. (45) in Eq (43),

$$\psi^* = - \left[ \frac{{}^\infty q_{1s} \kappa^2}{(\kappa r_i + 1) \exp(-\kappa r_i)} \right] \frac{\exp(-\kappa r)}{r} \quad (46)$$

Eq. (2) i.e.  $\rho_e^* = -\psi^*$  gives,

$$\rho_e^* = \left[ \frac{{}^\infty q_{1s} \kappa^2}{(\kappa r_i + 1) \exp(-\kappa r_i)} \right] \frac{\exp(-\kappa r)}{r} \quad (47)$$

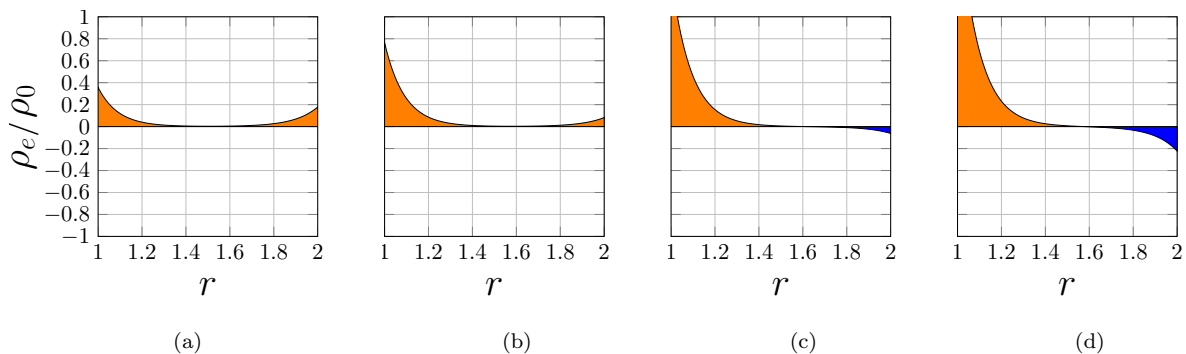


FIG. 2. (Color online) Charge density distribution within a fluid, bounded between two concentric spheres. We vary the potential difference between the boundaries i.e. ‘ $v$ ’, keeping other parameters constant e.g.  $\kappa = 10.0$ ;  $q_{1s} = 0.1$ ; (scaled) radii of inner and outer spheres are  $r_i = 1$  and  $r_o = 2$ . (a)  $v = 0$ ; excess charges accumulate near boundaries. (b)  $v = 0.6$ ; an applied voltage redistributes charges. (c)  $v = 1.5$ ; strong voltage segregates negative charges even if  $q_{1s} > 0$ . (d)  $v = 2.5$ ; stronger voltage makes higher segregation. Please compare this figure with figure (1) in Ref. [11] and figure (2) in Ref. [6]:

#### D. Results and discussions

##### a. Domain bounded between two concentric spheres:

Using Eq. (34) we plot  $\rho_e^*$  vs  $r$  in Fig. (2); to compare the results, we use the same range for  $r$  that was used in Ref. [6]:  $[1 \leq r \leq 2]$  i.e. we took  $a = R_i$  and  $R_o = 2R_i$ , so that  $r_i = 1$ , and  $r_o = 2$ . The description of the plots are similar to that of the rectangular or the cylindrical geometry (Ref. [6, 11]); the non-zero net charge in the domain gather near the two boundaries. The charges distribute differently when the potential difference between the boundaries changes; positive and negative charges move towards the boundaries that minimizes their potential energies. For a given value of  $q_{1s}$ , the charged layers near the inner and the outer boundaries may be of opposite polarities when the voltage is very high.

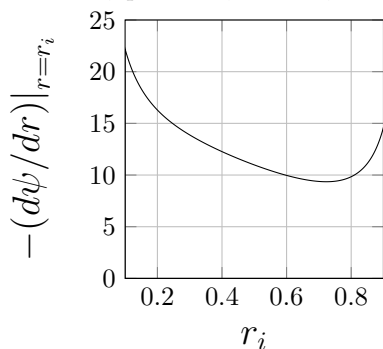


FIG. 3. The variation of the electric field at the surface of the inner sphere when the inner-sphere-radius  $r_i$  is varied, keeping the outer-sphere-radius  $r_o$  fixed; the domain of analysis is bounded between two concentric spheres of radii  $r_o$  and  $r_i$ , filled with ionic liquids.

Next, using Eq. (17), we plot  $(-d\psi/dr)|_{r=r_i}$  vs.  $r_i$  in Fig. (3) for  $0.1 \leq r_i \leq 0.9$ ; other parameters are kept at constant values:  $\kappa = 10$ ,  $q_{1s} = 0.1$ ,  $v = 0$ ,  $r_o = 1$ . Physically, we keep the size of the bigger sphere fixed and vary the size of the inner sphere to study how the electric field on its surface (i.e. at  $r = r_i$ ) varies with the size. The field is very high for small sphere (e.g. when  $r_i = 0.1$ ), as we increase  $r_i$ , the field decreases monotonically upto quite a large value of  $r_i$  ( $\sim 0.75$  for the particular set of parameters that are kept constant), then started increasing again with  $r_i$ .

In this context, we mention an analogous case where the sharp parts of a charged metallic object are associated with much higher electric fields than the other parts; see Feynman et al [21], (pp. 6-13 sec. 6-11, ‘High-voltage breakdown’); it says that the charges on the surface of a conductor tend to spread out as much as possible and hence a significant number of charges accumulate on the tip of a sharp point, because this tip is farthest from most part of the surface. Even a small quantity of charge produces high charge-density due to the small size of the tip, which causes high electric field just outside this tip.

However, for metallic objects, free charges reside on its *surface*, and the charge density at the surface is used to calculate the electric field; unlike this, in electrolytic solutions, the charges distribute over a *volume*, and the *gradient* of the charge density is used to calculate the electric field (in the PB model). However, like the metallic case, a significant number of charges accumulate near the smaller sphere, because it is the farthest place from most of the surface available in the domain i.e. the bigger sphere.

Beyond a certain critical value of  $r_i$ , the electric field at the inner surface starts to increase with  $r_i$ . This happens because the inner surface is now very close to the outer one, so that the charges at the outer surface have strong influence at the inner surface. When the two surfaces are very close the two layers may overlap and the electric

filed increases very rapidly with  $r_i$ .

For the distribution inside a finite, single sphere, see Sec. IIB, when  ${}^0q_{1s} = 0$ , we have  $\rho_e^* = 0$  everywhere according to Eq. (47). When  ${}^0q_{1s} \neq 0$ , we have  $\rho_e^*$  finite everywhere, even at the center of the sphere, since  $\lim_{r \rightarrow 0} (\sinh(\kappa r)/r) \rightarrow 1$ . However, the magnitude of  $\rho_e^*$  is higher near the surface of the sphere than its central region.

We have derived the distribution outside a single sphere in a semi-infinite domain in Sec. IIC. When  ${}^\infty q_{1s} = 0$ , we have  $\rho_e^* = 0$  everywhere according to Eq. (47). When  ${}^\infty q_{1s} \neq 0$ , the charges accumulate near the spherical surface; the magnitude of  $\rho_e^*$  falls rapidly with distance.

The above formulae of  $\rho_e^*$  for different spherical geometries and a few of their consequences will be very much useful when we design equipments and explain relevant natural processes.

### III. ACKNOWLEDGMENT

This paper is a continuation of the work that I had started at IISER-Kolkata; hence I have used their affiliation, although I am not attached to them presently. Thanks to Abhijit Sarkar, Sujata Sarkar and my parents for their financial supports. Thanks to Indian Association for the Cultivation of Science; I have used their library facilities.

### IV. NOTE

The work is being uploaded to **vixra.org**

- 
- [1] P. Debye and E. Huckel, *Physikalische Zeitschrift* **24**, 185 (1923).
- [2] R. B. Schoch, J. Han, and P. Renaud, *Rev. Mod. Phys.* **80**, 839 (2008).
- [3] J. Lyklema, *Fundamentals of Interface and Colloid Science*, Vol. 2 (Academic, London, 1991).
- [4] N. Bukar, S. S. Zhao, D. M. Charbonneau, J. N. Pelletier, and J.-F. Masson, *Chem. Commun.* **50**, 4947 (2014).
- [5] F. Fogolari, A. Brigo, and H. Molinari, *J. Mol. Recognit.* **15**, 377 (2002).
- [6] R. Chakraborty, "Solution to Poisson Boltzmann equation in semi-infinite and cylindrical geometries," <http://vixra.org/abs/1511.0057> (2015).
- [7] R. Chakraborty, "Electric triple-layer theory," <http://vixra.org/abs/1405.0354> (2014).
- [8] R. Chakraborty, "Electric triple-layer theory," (2014), *Phys. Rev. E* (unpublished).
- [9] R. Chakraborty, "Mystery of missing co-ions solved," <http://vixra.org/abs/1408.0186> (2014).
- [10] R. Chakraborty, "Physical solution of Poisson-Boltzmann equation," <http://www.vixra.org/abs/1408.0093> (2014).
- [11] R. Chakraborty, "Debye length cannot be interpreted as screening or shielding length," <http://www.vixra.org/abs/1502.0051> (2015).
- [12] R. Chakraborty, "Debye length cannot be interpreted as screening or shielding length," (2015), *J. Colloid & Interface Sci.* (unpublished; Manuscript Number: JCIS-15-1110, submitted formally through online submission system, if the editor cannot provide it, please write the author).
- [13] R. Chakraborty, "Debye length cannot be interpreted as screening or shielding length," (2015), *J. Colloid & Interface Sci.* (unpublished; Manuscript Number: JCIS-15-1110: please see the revised version sent to the editors through e-mail; in case the editors cannot provide it please contact the author).
- [14] E. J. W. Verwey and J. T. G. Overbeek, *Theory of the Stability of Lyophobic Colloids* (Elsevier Publishing Company Inc., New York, Amsterdam, London, Brussels, 1948).
- [15] Z. Yao, M. J. Bowick, and X. Ma, "The electric double layer structure around charged spherical interfaces," <https://arxiv.org/pdf/1110.5309.pdf> (2012).
- [16] A. Phan, D. Tracy, T. L. H. Nguyen, V. Nguyen Ai, T. Phan, and T. Nguyen, *The Journal of Chemical Physics* **139**, 244908 (2013).
- [17] E. W. Weisstein, "Spherical coordinates," <http://mathworld.wolfram.com/SphericalCoordinates.html>, ( From *MathWorld*—A Wolfram Web Resource).
- [18] G. B. Arfken and H. J. Weber, *Mathematical Methods for Physicists*, 4th ed. (Academic Press, Inc., San Diego, USA, 1995).
- [19] R. Chakraborty, "Debye length cannot be interpreted as screening or shielding length," (2015), *J. Phys. : Cond. Mat.* (unpublished).
- [20] "List of integrals of hyperbolic functions," [https://en.wikipedia.org/wiki/List\\_of\\_integrals\\_of\\_hyperbolic\\_functions](https://en.wikipedia.org/wiki/List_of_integrals_of_hyperbolic_functions).
- [21] R. Feynman, R. B. Leighton, and M. Sands, *The Feynman Lectures on Physics*, Vol. 2 (Narosa Publishing House, New Delhi, India, 1964).